

Ringdown Spectroscopy of Rotating Black Holes Pierced by Cosmic Strings

Mark Ho-Yeuk Cheung,^{1,*} Levi Wing-Hei Poon,^{1,*} Adrian Ka-Wai Chung,^{1,2} and Tjonne Guang Feng Li¹

¹*Department of Physics, The Chinese University of Hong Kong, Shatin, N.T., Hong Kong*

²*Theoretical Particle Physics and Cosmology Group,
Department of Physics, Kings College London*

Multiple gauge theories predict the presence of cosmic strings with different mass densities $G\mu$. We derive an equation governing the perturbations of a rotating black hole pierced by a straight, infinitely long cosmic string along its axis of rotation and calculate the quasinormal-mode frequencies of such a black hole. We then carry out parameter estimation on the first detected gravitational-wave event, GW150914, by hypothesizing that there is a string piercing through the remnant, yielding a constraint of $G\mu < 3.8 \times 10^{-3}$ at the 90% confidence interval with a comparable Bayes factor with a string-less analysis. In contrast to existing studies which focus on the mutual intersection of cosmic strings, or the cosmic string network, our work focuses on the intersection of a cosmic string with a black hole.

I. INTRODUCTION

The detection of gravitational wave events by the Advanced LIGO and VIRGO detectors [1–8] has opened a new window in terms of astrophysical observations. Not only is it now possible to detect black hole and neutron star merger events, but also to infer the properties of the merging objects by analysing their gravitational-wave signals. In particular, analysing the quasinormal-mode frequencies (QNMFs) [9–11] of the decaying waves at the final ringdown stage of a binary black-hole merger event could help infer the different parameters that characterize the remnant black hole. A cosmic string hair of black holes might also be probed in the same way.

Cosmic strings are hypothetical topological defects predicted by some gauge theories and could have formed during cosmological phase transition in the early universe [12, 13]. Efforts have been made to search for cosmic strings directly, or to constrain their mass density μ by analyzing the cosmic microwave background [14–18], stochastic gravitational-wave background [19–25], by considering their lensing effects [26–29] and bursts of gravitational wave produced by cosmic string cusps or kinks [30, 31]. The most stringent constraint put on the cosmic string network is $G\mu/c^2 < 1.5 \times 10^{-11}$ [24], while it is estimated that this constraint can be pushed to $G\mu/c^2 < 10^{-17}$ with LISA [32], where G is the gravitational constant.

Other than existing within its own network, cosmic strings might also be found piercing through black holes. Such a configuration could form when a black hole with non-zero magnetic charge cools below the transition temperature [33], or when a primordial black hole forms around a string [34]. It has

been shown that cosmic strings can be stably supported by black hole horizons, giving rise to long range black hole hair [35–45], possibly serving as a counter-example to the no hair theorem [46, 47]. If the black hole is rotating, the string will align with the axis of rotation of the black hole at equilibrium [45], hence we call such a black hole a Kerr-string black hole. The QNMFs of a non-rotating Schwarzschild-string black hole have been calculated in Refs. [48, 49], but not for the case of a Kerr-string black hole with non-zero angular momentum.

In this paper, we will show that cosmic string hair of a Kerr black hole would affect its ringdown waveforms, providing a way to search for cosmic strings by gravitational-wave detection and ringdown-spectroscopy analysis. The QNMFs of a Kerr-string black hole are first calculated by solving a modified Teukolsky equation that takes the effect of the cosmic string into account. Then, we will constrain the mass density of cosmic strings piercing through the remnant black hole formed in the merger event GW150914 detected by LIGO [1] with its ringdown signal, as well as discuss the degeneracies between different parameters in our analysis.

Throughout the remainder of this paper, we will adopt the $(+, -, -, -)$ convention and units where $G = c = 1$ will be used. However, to remain consistent with the literature, we will keep the G in front of μ .

II. THE PERTURBATION EQUATION

The metric of a Kerr-string black hole, consisting of a black hole with mass M and specific angular momentum a pierced by a cosmic string of infinite length along the axis of rotation with dimensionless

* These authors contributed equally.

mass density $G\mu \ll 1$, is given by [50]

$$ds^2 = \frac{\Delta \Sigma}{\Gamma} dt^2 - \frac{\Gamma \sin^2 \theta}{\Sigma} \left(b d\phi - \frac{2aMr}{\Gamma} dt \right)^2 - \Sigma \left(\frac{dr^2}{\Delta} + d\theta^2 \right), \quad (1)$$

where $b = 1 - 4G\mu$, $\Sigma = r^2 + a^2 \cos^2 \theta$, $\Delta = r^2 + a^2 - 2Mr$ and $\Gamma = (r^2 + a^2)^2 - \Delta a^2 \sin^2 \theta$. This metric can be obtained by introducing an azimuthal angular deficit of $8\pi G\mu$ on ϕ to the Kerr metric, and it remains a Petrov type D vacuum metric, suggesting that the Teukolsky formalism of treating black hole perturbation could be applied to the system.

Locally, Eq. (1) is equal to the Kerr metric with ϕ rescaled to $b\phi$, so the perturbation equation for

Eq. (1) can be obtained by repeating Teukolsky's computation [51] with the following null tetrad:

$$l^\mu = \frac{1}{\Delta} \left\langle r^2 + a^2, \Delta, 0, \frac{a}{b} \right\rangle, \quad (2)$$

$$n^\mu = \frac{1}{2\Sigma} \left\langle r^2 + a^2, -\Delta, 0, \frac{a}{b} \right\rangle, \quad (3)$$

$$m^\mu = \frac{1}{\sqrt{2}(r + ia \cos \theta)} \left\langle ia \sin \theta, 0, 1, \frac{i}{b \sin \theta} \right\rangle, \quad (4)$$

$$\bar{m}^\mu = \frac{1}{\sqrt{2}(r - ia \cos \theta)} \left\langle -ia \sin \theta, 0, 1, \frac{-i}{b \sin \theta} \right\rangle. \quad (5)$$

Then, the master equation for black holes pierced by cosmic strings is derived to be

$$\begin{aligned} & \left[\frac{(r^2 + a^2)^2}{\Delta} - a^2 \sin^2 \theta \right] \frac{\partial^2 \Psi}{\partial t^2} + \frac{4Mar}{\Delta} \frac{\partial^2 \Psi}{\partial t \partial \phi} + \frac{1}{b^2} \left[\frac{a^2}{\Delta} - \frac{1}{\sin^2 \theta} \right] \frac{\partial^2 \Psi}{\partial \phi^2} \\ & - \Delta^{-s} \frac{\partial}{\partial r} \left(\Delta^{s+1} \frac{\partial \Psi}{\partial r} \right) - \frac{1}{\sin \theta} \frac{\partial}{\partial \theta} \left(\sin \theta \frac{\partial \Psi}{\partial \theta} \right) - \frac{2s}{b} \left[\frac{a(r - M)}{\Delta} + i \frac{\cos \theta}{\sin^2 \theta} \right] \frac{\partial \Psi}{\partial \phi} \\ & - 2s \left[\frac{M(r^2 - a^2)}{\Delta} - r - ia \cos \theta \right] \frac{\partial \Psi}{\partial t} + (s^2 \cot^2 \theta - s) \Psi = 4\pi \Sigma T. \end{aligned} \quad (6)$$

This is equivalent to the original Teukolsky equation with ϕ replaced by $b\phi$.

III. QUASINORMAL MODE FREQUENCIES

By considering a vacuum perturbation (i.e., $T = 0$), we can compute the QNMFs using Leaver's method of continued fraction [11, 52]. Analogous to Teukolsky's computations [51], by putting $\Psi = e^{i(m\phi - \omega t)} R(r) S(\theta)$, Eq. (6) is separable into a radial equation and an angular equation:

$$\begin{aligned} & \Delta^{-s} \frac{d}{dr} \left(\Delta^{s+1} \frac{dR}{dr} \right) \\ & + \left[\frac{K^2 - 2is(r - M)K}{\Delta} + 4is\omega r - \lambda \right] R = 0, \end{aligned} \quad (7)$$

$$\begin{aligned} & \frac{1}{\sin \theta} \frac{d}{d\theta} \left(\sin \theta \frac{dS}{d\theta} \right) + \left[(a\omega \cos \theta - s)^2 \right. \\ & \left. - \left(\frac{m/b - s \cos \theta}{\sin \theta} \right)^2 - s^2 + s - A \right] S = 0, \end{aligned} \quad (8)$$

where $K = (r^2 + a^2)\omega - am/b$, $\lambda = A + a^2\omega^2 - 2am\omega/b$ and A is a separation constant. Effectively,

the inclusion of a cosmic string amounts to changing m to m/b in Eq. (7) and Eq. (8), the QNMFs can hence be computed by changing the value of m in Leaver's algorithm.

Fig. 1 shows the dependence of the $(n, l, m) = (0, 2, 2)$ overtone frequency on $G\mu$ at various values of the spin parameter a/M . A bluer hue represents a larger value of $G\mu$ and a redder hue represents a larger value of a . Both the frequency and the decay rate of gravitational wave emissions increase with the mass density of the cosmic string. Notably, an increasing spin and an increasing $G\mu$ drive the $(0, 2, 2)$ overtone QNMFs in different directions. This suggests that parameter estimation through ringdown analysis is possible. Moreover, none of the common alternative gravitational theories that would affect the QNMFs increase both $|\tilde{\omega}^{\text{Im}}|$ and $|\tilde{\omega}^{\text{Re}}|$ together [53–57], so parameter estimation on $G\mu$ done with the QNMFs will not be degenerate with these theories.

Interesting trends are found in the QNMFs of black holes with cosmic strings. In the Schwarzschild case ($a = 0$), the separation constant is given by $A_{lm} = l(l+1) - s(s+1)$ [51]. With the effect of a cosmic string included, for modes with $n = 0$ and $l = m = 2, 3, 4$, it is noticed that the separation constant is modified to $A_{lm} = (l/b)(l/b+1) - s(s+1)$

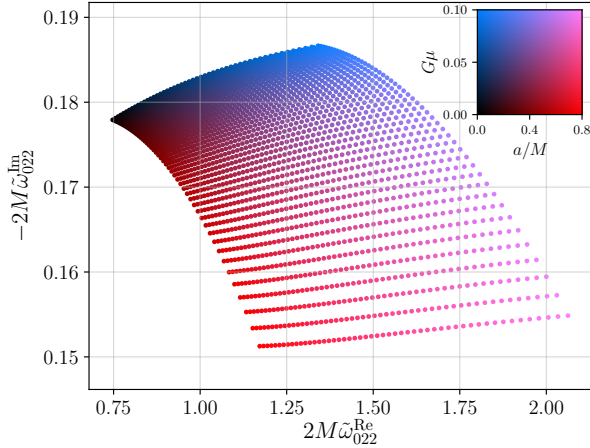


FIG. 1. The real and imaginary parts of the $(n, l, m) = (0, 2, 2)$ overtone QNMFs for $0 \leq G\mu \leq 0.1$ and $0 \leq a/M \leq 0.8$. Blueness and redness represent the values of $G\mu$ and a respectively. The dots are evenly spaced in $G\mu$ and a . This shows that increasing $G\mu$ increases the magnitudes of both the real and imaginary parts of the QNMFs $\tilde{\omega}_{022}$.

when $a = 0$ and that $\omega^{\text{Re}}(a, G\mu) \approx \omega^{\text{Re}}(a, 0)/b$. Such a relation is not present in modes with $l \neq m$.

The QNMFs for each nlm overtone was fitted to a quadratic function in $G\mu$:

$$\begin{aligned} \tilde{\omega}_{nlm}(a, G\mu) &= \tilde{\omega}_{nlm}(a, 0) \\ &+ \tilde{\omega}_{nlm}(0, 0)[\tilde{c}_1(a)G\mu + \tilde{c}_2(a)(G\mu)^2]. \end{aligned} \quad (9)$$

The real and imaginary parts of $\tilde{c}_1(a)$ and $\tilde{c}_2(a)$ were then fitted to the form $k_1 - k_2(1 - a/M)^{k_3}$ as motivated by Ref. [58]. For the $(0, 2, 2)$ mode, which is the dominant mode in GW150914, the maximum error of the fit over the range $0 \leq G\mu \leq 0.1$, $0 \leq a/M \leq 0.95$ in the real and imaginary parts of the QNMFs is about 0.8% and 1.4% respectively. Table I shows the numerical values of the coefficients for this mode.

$f(a)$	k_1	k_2	k_3
$\text{Re}\{\tilde{c}_1(a)\}$	10.1	5.73	0.223
$\text{Im}\{\tilde{c}_1(a)\}$	2.34	1.43	0.289
$\text{Re}\{\tilde{c}_2(a)\}$	108	77.7	0.180
$\text{Im}\{\tilde{c}_2(a)\}$	60.7	53.4	0.0503

TABLE I. Fitted coefficients for $f(a) = k_1 - k_2(1 - a/M)^{k_3}$ for different $f(a)$ of the $(0, 2, 2)$ mode, where $f(a)$ are the real and imaginary parts of coefficients appearing in a quadratic of the QNMFs to $G\mu$.

Fig. 2 plots the ringdown waveforms of a Kerr-string black holes of different $G\mu$. The waveforms are assumed to be generated from a black hole

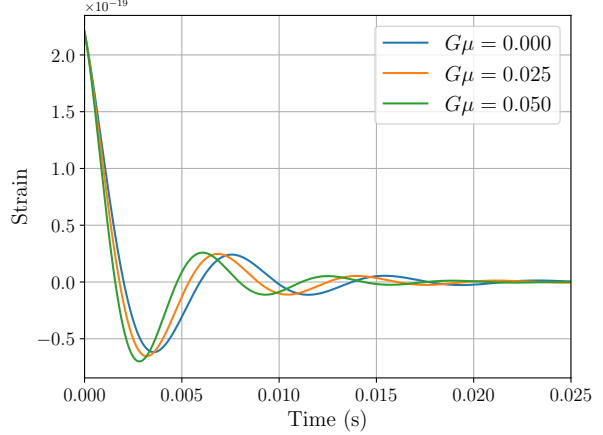


FIG. 2. Ringdown waveforms generated by Kerr-string black holes with different $G\mu$. Only the $(0, 2, 2)$ and $(1, 2, 2)$ modes are used in the generation of the waveforms. The frequency of QNM oscillation increases with $G\mu$ while the lifetime decreases slightly.

merger event where the $(n, l, m) = (0, 2, 2)$ and $(1, 2, 2)$ modes are dominant in the ringdown signal, and the mass of the final black hole M_f and final spin parameter a_f are the same for all the waveforms. Using two or more modes instead of one, we can ensure that our waveform has four degrees of freedom in its QNMFs, so it can carry information about all three parameters M , a and $G\mu$. Altering $G\mu$ would induce a change in the shape of the waveform, and the higher the value of $G\mu$, the more the waveform deviates from that from a system without a cosmic string.

Before making use of the QNMFs fits to constrain $G\mu$ with real data, it would be insightful to look into possible degeneracies between M_f or a_f with $G\mu$. We do this by considering the match between two waveforms, one with fixed parameters and $G\mu = 0$, the other with non-zero $G\mu$ and varying M_f or a_f . The match between waveforms is defined by

$$\text{match}[h_1, h_2] = \frac{\langle h_1 | h_2 \rangle}{\sqrt{\langle h_1 | h_1 \rangle \langle h_2 | h_2 \rangle}}, \quad (10)$$

with

$$h_1 \equiv h_1(M_{f1}, a_{f1}, G\mu_1; t), \quad (11)$$

$$h_2 \equiv h_2(M_{f2}, a_{f2}, G\mu_2; t), \quad (12)$$

and

$$\begin{aligned} \langle h_1 | h_2 \rangle &= \\ &\int_{t_i}^{t_f} h_1^*(M_{f1}, a_{f1}, G\mu_1; t) h_2(M_{f2}, a_{f2}, G\mu_2; t) dt, \end{aligned} \quad (13)$$

where $h_1(M_{f1}, a_{f1}, G\mu_1; t)$ and $h_2(M_{f2}, a_{f2}, G\mu_2; t)$ correspond to ringdown waveforms in the time domain with different parameters M_f , a_f and $G\mu$, and $*$ denotes complex conjugation. The starting and ending time of the ringdown signals are set to be $t_i = 0$ s and $t_f = 0.030$ s for matching.

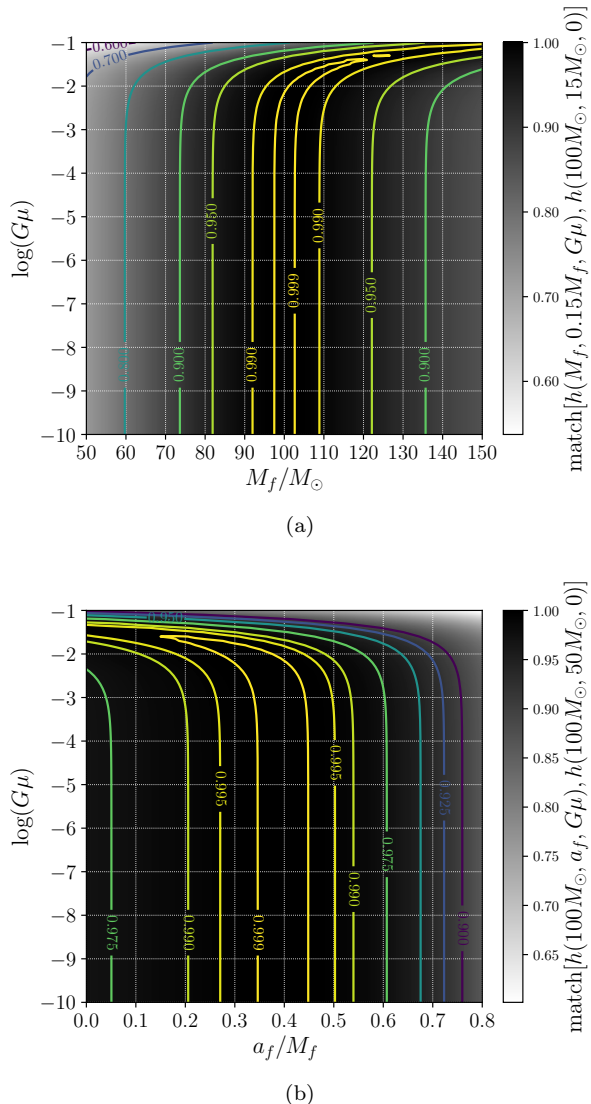


FIG. 3. Contour plots of match between waveforms with different parameters to test the degeneracy of $G\mu$ with M_f and a_f . (a): Match between a fixed string-less waveform with M_f fixed at $100M_\odot$ and one with variable $G\mu$ and M_f (both with a_f/M_f fixed at 0.67). Degeneracy is observed for $\log G\mu > -3$, where a string-less waveform will look like a string-carrying waveform with a higher mass. (b): Match between a fixed string-less waveform with $a_f/M_f = 0.4$ and one with variable $G\mu$ and a_f (both with M_f fixed at $100M_\odot$). Similar to (a), there is degeneracy observed for $\log G\mu > -3$, but with a string-less waveform looking like a string-carrying waveform with less spin.

The match between the waveforms $h(M_f, 0.67M_f, G\mu)$ and $h(100M_\odot, 67M_\odot, 0)$ is plotted in Fig. 3a (calculated with the PYCBC software [59]). By varying M_f and $G\mu$, it is found that the two parameters are degenerate in the $\log(G\mu) > -3$ regime. Nonetheless, for sufficiently high values of the match, the majority of the contour area is still centered at $M_f = 100M_\odot$ and terminates at some high value of $\log(G\mu)$, meaning that it is still possible to constrain $G\mu$ by matched filtering without affecting too significantly the parameter estimation of M_f . Similarly, Fig. 3b test the degeneracy of $G\mu$ with a_f . Again, there is degeneracy in the high $\log(G\mu)$ regime, which will cause a string-less waveform to look like a string-carrying waveform with less spin. This will cause the constrain on $G\mu$ to be less tight.

IV. RESULTS

With the QNMFs of the Kerr-string black hole calculated, we will put a constraint on $G\mu$ of the GW150914 system by assuming that its final black hole is a Kerr-string black hole. Parameter estimation is carried out with the PYRING pipeline introduced in Ref. [60].

If GW150914 were a merger of primordial black holes (as suggested by [61, 62]), it might be possible for at least one of the black holes in the binary to hold cosmic strings. When this Kerr-string black hole merges with the other black hole, the remnant will also be a Kerr-string black hole and it will emit a ringdown signal characterized by the parameters M_f , a_f and $G\mu$. Thus, we can hypothesize that the ringdown signal of GW150914 comes from a Kerr-string black hole and constrain the mass density of the hypothetical string piercing through it.

As mentioned earlier, we will have to use at least two modes to estimate the three parameters M , a and $G\mu$. We might have chosen to use the $(0, 2, 2)$ and $(0, 2, 1)$ modes in theory due to them being the two most excited modes of GW150914 [63], but the large $G\mu$ $(0, 2, 1)$ QNMFs have values too close to those of low $G\mu$ $(0, 2, 2)$, which will cause the pipeline to falsely recognize high $G\mu$ waveforms in the data. Therefore, the $(0, 2, 2)$ and $(1, 2, 2)$ ringdown modes are used. The prior distribution for $\log(G\mu)$ and start time are respectively set to be a uniform distribution within $[-10, -1]$ and $[10, 20]M$ [64, 65], where $M = 68M_\odot$ is the reported median value of the final mass in Ref. [66]. The prior distributions of other parameters as well as the treatment of noise of the LIGO data are the same as those in Ref. [60].

Figure 5(a) shows the contour plot of the final

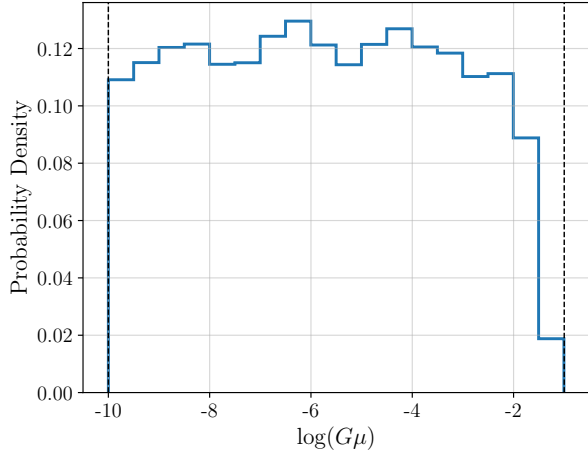


FIG. 4. The posterior distribution of $\log(G\mu)$ for the GW150914 event. The shape of the distribution resembles that of a step function. There is a sharp drop near $\log(G\mu) = -2$. We obtain a constraint of $G\mu < 3.8 \times 10^{-3}$ at the 90% confidence level. The prior bounds are marked with dotted lines.

spin parameter a_f/M_f and final mass M_f , with the median values estimated by a full IMR analysis [1] marked by two black dotted lines. When compared to the same graph for an analysis without the parameter estimation of $G\mu$ [Fig. 5(b)], it can be seen that the plots have generally the same shape. However, the distribution in Fig. 5(a) leans more to the larger M_f side, while the degeneracy in a_f is not clearly seen. Fig. 5(a) also shows a slightly wider spread in M_f , but the spread in a_f is reduced. Fig. 6 plots explicitly the three dimensional posterior of M_f , a_f and $G\mu$. It can be clearly seen that the higher $G\mu$ points lie to the higher M_f and smaller a_f side, agreeing with our waveform degeneracy analysis in Sec. III.

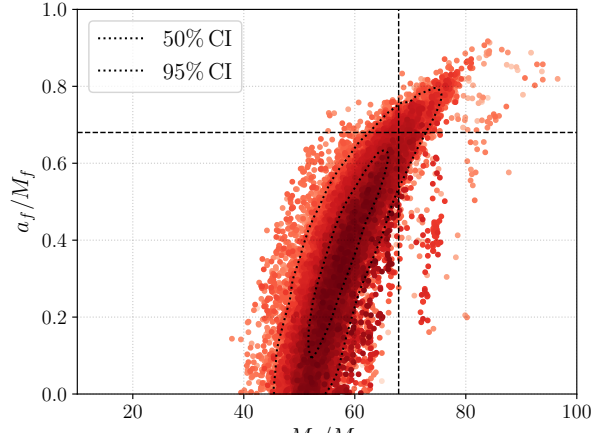
Figure 7 shows a corner plot for M_f , a_f and $\log(G\mu)$. As evident from the absence of clear trend lines in the contour plots of $\log(G\mu)$ against M_f or a_f , the degeneracy between the effects of $G\mu$ and those of M_f or a_f are not too significant.

This three-parameter analysis gives a Bayes factor of $\log B = 59.3$. When compared with $\log B = 59.1$ for an analysis with only M_f and a_f , this suggests that the two models are similar in plausibility.

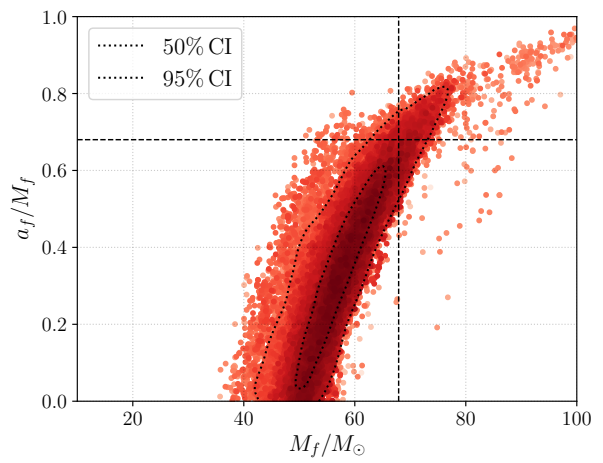
V. DISCUSSION AND CONCLUSIONS

A. Assumptions Made

For the analysis using QNMFs obtained from Eq. (6) to be valid, three conditions need to be sat-



(a)



(b)

FIG. 5. Contour plots of the final mass M_f and spin parameter a_f/M_f in the generated posterior data set for GW150914 for analysis (a) with and (b) without an additional parameter estimation on $G\mu$. The vertical and horizontal black dotted lines represent the published median values for the detector-frame final mass M_f and final spin a_f/M_f of the GW150914 event given in Ref. [67]. The shape of the two plots are similar, except that the plot in Fig. (a) is more biased towards larger M_f , while the spread in a_f is smaller.

isfied:

1. The spins of the black holes during the inspiral phase are aligned with the orbital angular momentum vector.
2. The string is infinitely long and straight after the merger.
3. The string lies on the axis of rotation of the final black hole.

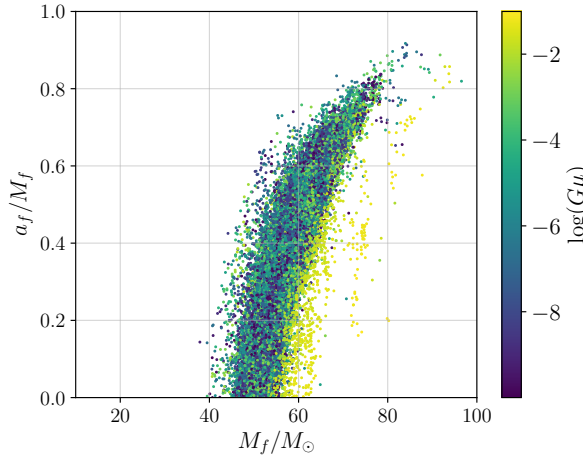


FIG. 6. Posterior plot of all three parameters M_f , a_f and $G\mu$. The yellow hue corresponds to points with higher $G\mu$, and they are located more towards the high M_f and low a_f side, agreeing with our waveform degeneracy analysis in Sec. III.

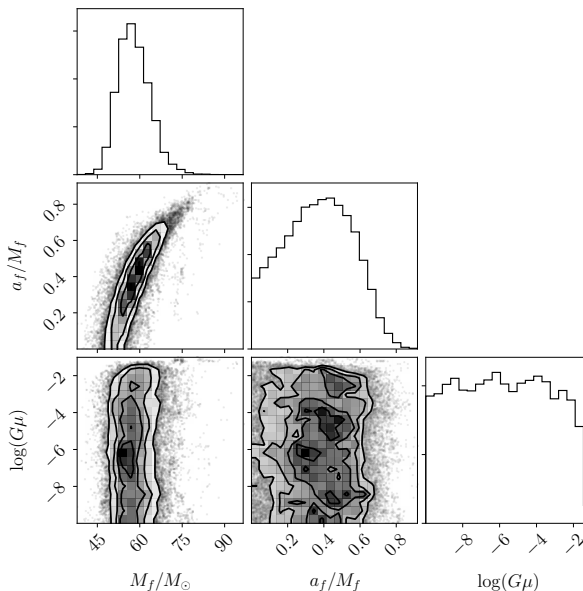


FIG. 7. A corner plot showing the posterior distribution of M_f , a_f and $\log(G\mu)$. Unlike the contour plot for a_f and M_f , no clear trend lines can be observed in the contour plots of $\log(G\mu)$ versus a_f and M_f .

(1) is necessary for (2) and (3): If (1) is not true, the spin of the Kerr-string black hole will precess, so the string will likely curl around itself, violating (2). Moreover, if the spins of the binary black holes are misaligned, the spin of the final black hole might also be misaligned with the string, violating (3). A rotating black hole pierced by a cosmic string would gradually approach an equilibrium position where

the string aligns with the rotational axis of the black hole [45]. We assumed that the time scale for the approach to this equilibrium is much shorter than the time scale for merger and ringdown so that the ringdown signal is not contaminated by the signal from this stabilization.

In reality, as disturbances travel at a finite speed on the string, even if the spins of the binary black holes and the total angular momentum of the black hole merger are aligned perfectly, the string will spiral with the black holes during the inspiral phase. However, as the orbital radius of the black holes decreases, the string will steadily approach its final configuration, in which it passes through the center of mass of the system (i.e., the center of the final black hole) and aligns with the system's angular momentum, so it could stabilize soon after the merger. In that case, assumptions (2) and (3) can be satisfied locally and approximately.

In the future, work may be done to relax these assumptions and consider more general configurations of the Kerr-string black hole. In particular, numerical simulation of the disturbances to the Kerr-string black hole during the inspiral and merger phase will allow for a more comprehensive analysis of the ringdown signals emitted by such a system.

B. Comparison with Existing Results

Unlike our constraints, methods based on analysis of the cosmic microwave background or the stochastic gravitational wave background apply to entire cosmic string networks. The effects of the cosmic string network on the background spectrum are model-dependent since one must take the spatial arrangement and temporal evolution of the cosmic strings into account. Hence, the constraint so obtained will depend on the precise model used to simulate the cosmic string network (see, for example, Ref. [15]).

Our methods are more similar to searches for gravitational wave bursts or signs of lensing from cosmic strings in that these are methods of direct search. The constraint obtained only applies to a single event and a global constraint can only be obtained given models of event rates and arrangements of cosmic strings.

C. Conclusion

In conclusion, we showed that it is possible to constrain the mass density of cosmic strings piercing rotating black holes by analyzing its ringdown signal. Although the constraint on the GW150914 event is

less stringent than those obtained in Ref. [24], our work serves as a new way to constrain an individual cosmic string instead of the whole cosmic string network.

ACKNOWLEDGEMENTS

This research has made use of data, software and/or web tools obtained from the Gravitational Wave Open Science Center (<https://www.gw-openscience.org>), a service of LIGO Laboratory, the LIGO Scientific Collaboration and the Virgo Collaboration [68]. LIGO is funded by the U.S. National Science Foundation. Virgo is funded by the French Centre National de Recherche Scientifique (CNRS),

the Italian Istituto Nazionale della Fisica Nucleare (INFN) and the Dutch Nikhef, with contributions by Polish and Hungarian institutes.

The authors are indebted to valuable discussion among the Testing General Relativity (TGR) working group of LIGO. The authors are grateful to Gregorio Carullo, Xavier Siemens and Mairi Sakellariadou for their insightful comments on the manuscript. A.K.W.C. is supported by the Hong Kong Scholarship For Excellence Scheme (HKSES). The work described in this paper was partially supported by grants from the Research Grants Council of the Hong Kong (Project No. CUHK 24304317), The Croucher Foundation of Hong Kong, and the Research Committee of the Chinese University of Hong Kong.

[1] B. P. Abbott *et al.* (LIGO Scientific Collaboration and Virgo Collaboration), *Phys. Rev. Lett.* **116**, 061102 (2016).

[2] B. P. Abbott *et al.* (LIGO Scientific Collaboration and Virgo Collaboration), *Phys. Rev. Lett.* **116**, 241103 (2016).

[3] B. P. Abbott *et al.* (LIGO Scientific Collaboration and Virgo Collaboration), *Phys. Rev. Lett.* **118**, 221101 (2017).

[4] B. P. Abbott *et al.*, *The Astrophysical Journal Letters* **851**, L35 (2017).

[5] B. P. Abbott *et al.* (LIGO Scientific Collaboration and Virgo Collaboration), *Phys. Rev. Lett.* **119**, 141101 (2017).

[6] B. P. Abbott *et al.* (LIGO Scientific Collaboration and Virgo Collaboration), *Phys. Rev. Lett.* **119**, 161101 (2017).

[7] B. P. Abbott *et al.* (LIGO Scientific Collaboration and Virgo Collaboration), *Phys. Rev. X* **6**, 041015 (2016).

[8] B. P. Abbott *et al.* (LIGO, VIRGO, KAGRA Scientific Collaboration), *Living Rev. Rel.* **21**, 3 (2018), [Living Rev. Rel.19,1(2016)], arXiv:1304.0670 [gr-qc].

[9] H.-P. Nollert, *Class. Quantum Grav.* **16**, R159 (1999).

[10] K. D. Kokkotas and B. G. Schmidt, *Living Rev. Relativ.* **2**, 2 (1999).

[11] E. Berti, V. Cardoso, and A. O. Starinets, *Class. Quantum Grav.* **26**, 163001 (2009).

[12] A. Vilenkin and E. P. S. Shellard, *Cosmic strings and other topological defects* (Cambridge University Press, 2000).

[13] E. J. Copeland and T. Kibble, *Proc. R. Soc. A* **466**, 623 (2010).

[14] L. Pogosian and T. Vachaspati, *Phys. Rev. D* **60**, 083504 (1999).

[15] P. A. Ade, N. Aghanim, C. Armitage-Caplan, M. Arnaud, M. Ashdown, F. Atrio-Barandela, J. Aumont, C. Baccigalupi, A. Banday, R. Barreiro, *et al.*, *Astronomy & Astrophysics* **571**, A25 (2014).

[16] J. Lizarraga, J. Urrestilla, D. Daferrio, M. Hindmarsh, M. Kunz, and A. R. Liddle, *Phys. Rev. D* **90**, 103504 (2014).

[17] A. Lazanu, E. Shellard, and M. Landriau, *Phys. Rev. D* **91**, 083519 (2015).

[18] J. Lizarraga, J. Urrestilla, D. Daferrio, M. Hindmarsh, and M. Kunz, *J. Cosmol. Astropart. Phys.* **2016**, 042 (2016).

[19] A. Vilenkin, *Phys. Lett. B* **107**, 47 (1981).

[20] C. Hogan and M. Rees, *Nature* **311**, 109 (1984).

[21] R. H. Brandenberger, A. Albrecht, and N. Turok, *Nucl. Phys. B* **277**, 605 (1986).

[22] F. S. Accetta and L. M. Krauss, *Nucl. Phys. B* **319**, 747 (1989).

[23] C. Ringeval and T. Suyama, *J. Cosmol. Astropart. Phys.* **2017**, 027 (2017).

[24] J. J. Blanco-Pillado, K. D. Olum, and X. Siemens, *Phys. Lett. B* **778**, 392 (2018).

[25] J. J. Blanco-Pillado, K. D. Olum, and J. M. Wachter, “Energy-conservation constraints on cosmic string loop production and distribution functions,” (2019), arXiv:1907.09373 [astro-ph.CO].

[26] A. A. de Laix, L. M. Krauss, and T. Vachaspati, *Phys. Rev. Lett.* **79**, 1968 (1997).

[27] K. J. Mack, D. H. Wesley, and L. J. King, *Phys. Rev. D* **76**, 123515 (2007).

[28] D. B. Thomas, C. R. Contaldi, and J. a. Magueijo, *Phys. Rev. Lett.* **103**, 181301 (2009).

[29] S. Jung and T. Kim, arXiv preprint arXiv:1810.04172 (2018).

[30] T. Damour and A. Vilenkin, *Phys. Rev. D* **64**, 064008 (2001).

[31] B. Abbott, R. Abbott, T. Abbott, S. Abraham, F. Acernese, K. Ackley, C. Adams, R. Adhikari, V. Adya, C. Affeldt, *et al.*, *Phys. Rev. D* **100**, 024017 (2019).

[32] P. Auclair, J. J. Blanco-Pillado, D. G. Figueroa, A. C. Jenkins, M. Lewicki, M. Sakellariadou, S. Sanidas, L. Sousa, D. A. Steer, J. M. Wachter,

and S. Kuroyanagi, “Probing the gravitational wave background from cosmic strings with LISA,” (2019), arXiv:1909.00819 [astro-ph.CO].

[33] M. Aryal, L. Ford, and A. Vilenkin, Phys. Rev. D **34**, 2263 (1986).

[34] A. Vilenkin, Y. Levin, and A. Gruzinov, J. Cosmol. Astropart. Phys. **2018**, 008 (2018).

[35] M. Aryal, L. Ford, and A. Vilenkin, Phys. Rev. D **34**, 2263 (1986).

[36] A. Achúcarro, R. Gregory, and K. Kuijken, Phys. Rev. D **52**, 5729 (1995).

[37] F. Bonjour, R. Emparan, and R. Gregory, Phys. Rev. D **59**, 084022 (1999).

[38] M. Dehghani, A. Ghezelbash, and R. Mann, Nucl. Phys. B **625**, 389 (2002).

[39] M. Dehghani, A. Ghezelbash, and R. B. Mann, Phys. Rev. D **65**, 044010 (2002).

[40] A. Ghezelbash and R. Mann, Phys. Lett. B **537**, 329 (2002).

[41] A. Ghezelbash and R. Mann, Phys. Rev. D **65**, 124022 (2002).

[42] R. Gregory, D. Kubizňák, and D. Wills, J. High Energ. Phys. **2013**, 23 (2013).

[43] L. Nakonieczny and M. Rogatko, Phys. Rev. D **88**, 084039 (2013).

[44] R. Gregory, P. C. Gustainis, D. Kubizňák, R. B. Mann, and D. Wills, J. High Energ. Phys. **2014**, 10 (2014).

[45] D. Kubizňák, in *The Fourteenth Marcel Grossmann Meeting*, Vol. 2 (WORLD SCIENTIFIC, 2017) pp. 1828–1833, arXiv:1512.08807 [gr-qc].

[46] P. T. Chrusciel, in *results Proc. Joint AMS/CMS Conf. on Mathematical Physics and Differential Geometry (Vancouver)* ed J. Beem and K. Duggal (1994) pp. 23–49.

[47] J. D. Bekenstein, in *Proceedings of the Second International A.D. Sakharov Conference on Physics*, gr-qc/9605059 (1996) pp. 216–219.

[48] S. Chen, B. Wang, and R. Su, Int. J. Mod. Phys. A **23**, 2505 (2008).

[49] R. Sini and V. Kuriakose, Mod. Phys. Lett. A **24**, 2025 (2009).

[50] D. V. Gal'tsov and E. Masar, Class. Quantum Grav. **6**, 1313 (1989).

[51] S. A. Teukolsky, Phys. Rev. Lett. **29**, 1114 (1972).

[52] E. Leaver, Proceedings of the Royal Society A: Mathematical, Physical and Engineering Sciences **402**, 285 (1985).

[53] V. Cardoso and L. Gualtieri, Phys. Rev. D **80**, 064008 (2009).

[54] J. L. Blázquez-Salcedo, Z. Altaha Motahar, D. D. Doneva, F. S. Khoo, J. Kunz, S. Mojica, K. V. Staykov, and S. S. Yazadjiev, Eur. Phys. J. Plus **134**, 46 (2019).

[55] A. K.-W. Chung and T. G. F. Li, Phys. Rev. D **99** (2019), 10.1103/physrevd.99.124023.

[56] R. McManus, E. Berti, C. F. Macedo, M. Kimura, A. Maselli, and V. Cardoso, Phys. Rev. D **100** (2019), 10.1103/physrevd.100.044061.

[57] J. Bao, C. Shi, H. Wang, J.-d. Zhang, Y. Hu, J. Mei, and J. Luo, Phys. Rev. D **100** (2019), 10.1103/physrevd.100.084024.

[58] F. Echeverria, Phys. Rev. D **40**, 3194 (1989).

[59] A. Nitz, I. Harry, D. Brown, C. M. Biwer, J. Willis, T. D. Canton, C. Capano, L. Pekowsky, T. Dent, A. R. Williamson, M. Cabero, S. De, G. Davies, D. Macleod, B. Machenschalk, P. Kumar, S. Reyes, T. Massinger, F. Pannarale, M. T. Čipai, dfinstad, S. Fairhurst, S. Khan, A. Nielsen, shasvath, S. Kumar, idorrington92, L. Singer, H. Gabbard, and B. U. V. Gadre, “gwastro/pycbc: Pycbc release v1.14.2,” (2019).

[60] G. Carullo, W. Del Pozzo, and J. Veitch, Phys. Rev. D **99**, 123029 (2019).

[61] M. Sasaki, T. Suyama, T. Tanaka, and S. Yokoyama, Phys. Rev. Lett. **117**, 061101 (2016).

[62] S. Blinnikov, A. Dolgov, N. Porayko, and K. Postnov, J. Cosmol. Astropart. Phys. **2016**, 036 (2016).

[63] I. Kamaretsos, M. Hannam, and B. Sathyaprakash, Phys. Rev. Lett. **109** (2012), 10.1103/physrevlett.109.141102.

[64] S. Bhagwat, M. Okounkova, S. W. Ballmer, D. A. Brown, M. Giesler, M. A. Scheel, and S. A. Teukolsky, Phys. Rev. D **97** (2018), 10.1103/physrevd.97.104065.

[65] G. Carullo, L. van der Schaaf, L. London, P. T. Pang, K. W. Tsang, O. A. Hannuksela, J. Meidam, M. Agathos, A. Samajdar, A. Ghosh, and et al., Phys. Rev. D **98** (2018), 10.1103/physrevd.98.104020.

[66] B. P. Abbott *et al.* (LIGO Scientific Collaboration and Virgo Collaboration), Phys. Rev. Lett. **116**, 221101 (2016).

[67] B. P. Abbott, R. Abbott, T. Abbott, M. Abernathy, F. Acernese, K. Ackley, C. Adams, T. Adams, P. Adesso, R. Adhikari, et al., Phys. Rev. Lett. **116**, 241102 (2016).

[68] M. Vallisneri, J. Kanner, R. Williams, A. Weinstein, and B. Stephens, J. Phys.: Conf. Ser. **610**, 012021 (2015).